The Diamond Superconducting Quantum Interference Device

Soumen Mandal,[†,*] Tobias Bautze,[†] Oliver A. Williams,[‡,¶] Cécile Naud,[†] Étienne Bustarret,[†] Franck Omnès,[†] Pierre Rodière,[†] Tristan Meunier,[†] Christopher Bäuerle,[†,*] and Laurent Saminadayar[†,§]

[†]Institut Néel, CNRS and Université Joseph Fourier, 38042 Grenoble, France, [‡]Fraunhofer Institut Angewandte Festkörperphysik, Tullastrasse 72, 79108 Freiburg, Germany, [¶]School of Physics and Astronomy, Cardiff University, Queen's Buildings, The Parade, Cardiff CF24 3AA, United Kingdom, and [§]Institut Universitaire de France, 103 Boulevard Saint-Michel, 75005 Paris, France

ABSTRACT Diamond is an electrical insulator in its natural form. However, when doped with boron above a critical level (~0.25 atom %) it can be rendered superconducting at low temperatures with high critical fields. Here we present the realization of a micrometer-scale superconducting quantum interference device (μ-SQUID) made from nanocrystalline boron-doped diamond (BDD) films. Our results demonstrate that μ-SQUIDs made from superconducting diamond can be operated in magnetic fields as large as 4 T independent of the field direction. This is a decisive step toward the detection of quantum motion in a diamond-based nanomechanical oscillator.

KEYWORDS: diamond · SQUID · superconductivity · nanofabrication

Micrometer and nanometer scale superconducting quantum interference device (SQUIDS)[1] are extremely sensitive tools for magnetization measurements on the local scale and find applications in various fields of science such as scanning SQUID microscopy.[2] However, the present state of the art limits the utility of SQUIDs to magnetic fields well below a Tesla. Even though several attempts to realize micrometer scale superconducting quantum interference devices (μ-SQUIDs) from materials such as Nb_3Sn[3] or Nb_3Ge[4,5] with a high critical field have been realized, the demonstration of a device remaining operational at high magnetic fields has been elusive to date. In this context, diamond, when doped with boron above a critical level (~0.25 atom %) which results in a superconductor with very high critical field[6] is an extremely promising material. In addition, recent advances in diamond thin film growth technology have paved the way toward large scale processing of high quality devices.This recently discovered material not only enables us to make μ-SQUIDs capable of operating at fields as high as 4 T independent of the field direction, as reported in this paper, but also finds a potential application for ultrasensitive motion detection of diamond-based nanomechanical systems.[7]

The discovery of superconductivity in diamond[6,8−10] has opened the possibility to combine outstanding mechanical properties with superconductivity. Diamond is the archetype of superhard materials with the highest Young's modulus.[11,12] The main interest in such superhard superconducting materials comes from their possible application to high frequency nanomechanical systems. This high stiffness and the reduced mass of nanomechanical structures made out of diamond enable GHz vibration frequencies comparable with or higher than thermal energies at milliKelvin temperatures.[13] This opens the possibility of studying the quantum regime of such nanomechanical resonators.[14−16]

Advances in nanofabrication technology have made it possible to realize complex devices involving nanoelectromechanical components.[17,18] But in most cases the nanomechanical devices are compound/hybrid devices consisting of a superhard component with high Young's modulus generating high frequency resonators, and of a conducting component to reduce the transmission losses of the system. However, this conductive component increases the mass, degrades the mechanical properties, and thus reduces the overall quality factor of the device. In this context, boron- doped diamond turns out to be an excellent candidate for fabricating monolithic superconducting circuits involving nanomechanical systems with very high quality factor. One can then envision the direct integration of such nanomechanical systems into superconducting circuits such as SQUIDs[7] or superconducting resonators[19] for ultrasensitive motion detection.

RESULTS AND DISCUSSIONS

As a first step in this direction, we fabricated diamond μ-SQUIDS patterned from a 300 nm thick superconducting nanocrystalline diamond film. The boron doped diamond

* Address correspondence to soumen.mandal@gmail.com, bauerle@grenoble.cnrs.fr.

Received for review May 19, 2011 and accepted July 31, 2011.

Published online July 31, 2011
10.1021/nn2018396

films were grown by microwave plasma-enhanced chemical vapor deposition (MWPECVD) on seeded silicon 100 wafers with a silica buffer layer of 500 nm.[20] The thickness was monitored in *situ* with laser interferometry. The growth process has been discussed in detail elsewhere.[21] The diamond thin films were patterned using standard electron beam lithography. A thin nickel mask (65 nm) was deposited for subsequent highly anisotropic oxygen plasma etching.[22] Titanium–platinum–gold was deposited for the contact pads (Figure 1a), and the sample was annealed at 750 °C to ensure good ohmic properties.

We fabricated several similar devices as depicted in Figure 1 with various weak link designs of width of 250, 170, and 100 nm. These weak links serve as the Josephson junctions in the superconducting loop.[23,24] Here we mainly discuss data measured on a μ-SQUID with an area of 2.5 μm $\times$ 2.5 μm with two symmetric weak links (100 nm wide if not stated otherwise). Our low field measurements were performed in a ^{3}He closed cycle refrigerator with a base temperature of 400 mK, whereas the high field measurements have been undertaken in a dilution refrigerator at a temperature of 40 mK. The superconducting critical temperature of the bulk as well as the nanostructured diamond film was about 3 K as shown in Figure 2a.

The general characteristics of our μ-SQUIDS have been summarized in Figure 2. The current voltage ($I-V$) characteristic shows a thermal hysteresis[25,26] with a critical current of almost 1 μA and a retrapping current of about 0.55 μA. These parameters can be changed to some extent by tuning the geometrical aspects of the weak link. To demonstrate the performance of our diamond μ-SQUIDs we have measured the critical current oscillation as a function of perpendicular magnetic field. At low magnetic field we swept the current from a value slightly below the retrapping current until the switching of the SQUID was detected and recorded. This was repeated for different magnetic fields. The results for these experiments are shown in Figure 2c,d. An oscillation period of approximately 0.31 mT was recorded which corresponds to an effective SQUID surface area of 2.6 $\times$ 2.6 μm^2, in agreement with the geometrical dimensions of the μ-SQUID. The resulting modulation amplitude was about 15% for 100 nm wide weak links and around 5% for a 250 nm widths comparable to what is observed for Al and Nb μ-SQUIDs.[27] To probe the sensitivity of our μ-SQUID we repeated current switching measurements at a fixed magnetic field. Taking the full width at half-maximum and taking into account the sampling frequency we obtained a sensitivity of $4 \times 10^{-5}\Phi_0/(\mathrm{Hz})^{1/2}$, where Φ_0 is the superconducting flux quantum. This sensitivity is comparable to similarly designed μ-SQUIDS from frequently employed superconductors such as niobium or aluminum,[28] but a careful optimization of the SQUID design as well as material can lead to much higher

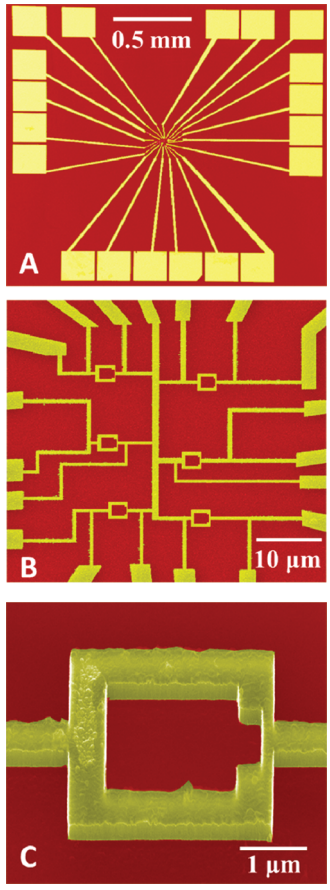

Figure 1. Scanning electron micrograph of the μ-SQUID circuit. (a) Image of the complete diamond circuit showing several pads for ohmic contacts. The total chip size is 2 mm $\times$ 2 mm. (b) Close-up view of a 50 $\times$ 50 μm^2 area in the middle of the sample. The circuit contains six μ-SQUIDs with different geometrical characteristics. (c) Tilted view of one of the μ-SQUIDs. The mean loop area of all the μ-SQUIDS is 2.5 $\times$ 2.5 μm^2. The thickness of the diamond film is 300 nm while the arms of the μ-SQUIDs are 500 nm wide. Two weak links of 170 nm in width and 250 nm in length can be identified.

sensitivities.[29] At present the sensitivity is only limited by the electronic measurement setup or external noise as the histograms are still symmetric and not limited by quantum fluctuations even at 40 mK. The main advantage of the diamond system is that superconductivity persists up to very high magnetic field (in our case more than 4 T). This is shown by the field dependence of the critical current as depicted in Figure 2f.

Various types of μ-SQUIDs have been reported in the literature, which are extremely sensitive magnetic flux detectors and currently used for scanning SQUID microscopy,[2,28] magnetization measurements in mesoscopic systems,[30,31] and in isolated molecules.[32] However, a severe drawback of these detectors is the narrow field range in which they are operable. In particular, μ-SQUID devices were operated at fields above 1 T only when the field is applied perfectly in the plane of the SQUID.[33] In addition, in such a parallel field configuration, the thickness of the superconducting layer

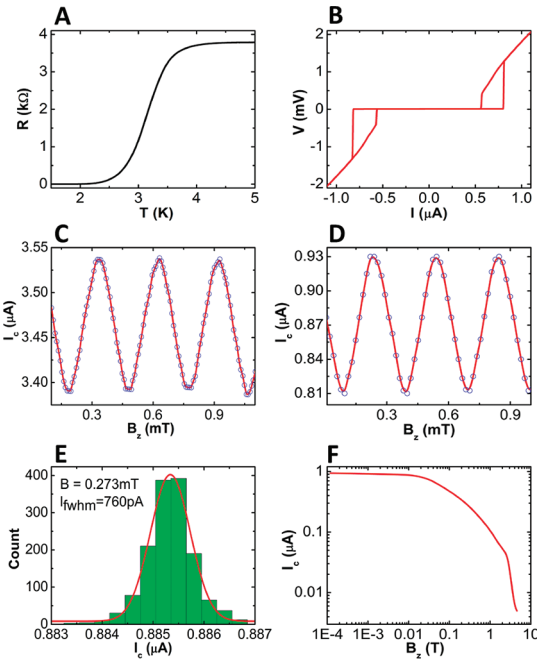

Figure 2. Characteristic features of the diamond μ-SQUID. (a) Superconducting transition of our μ-SQUID showing a transition temperature around 3 K which is close to the T_C of the diamond thin film. (b) Current−voltage characteristics of the μ-SQUID with 100 nm wide weak link. The $I-V$ curve is hysteretic with a critical current close to 1 μA and a retrapping current of about 0.55 μA. (c,d) Low field oscillation of the critical current as a function of magnetic field for a μ-SQUID with a width of a weak link of 170 and 100 nm, respectively. The oscillation period in both cases is around 0.31 mT. Red lines in the figures are guides to the eyes. (e) Histogram of the switching current of the μ-SQUID with a 100 nm wide weak link. The measurement was done by recording the switching current repetitively at a fixed magnetic field of 0.3 mT. (f) Field dependence of the critical current for the same μ-SQUID in perpendicular configuration.

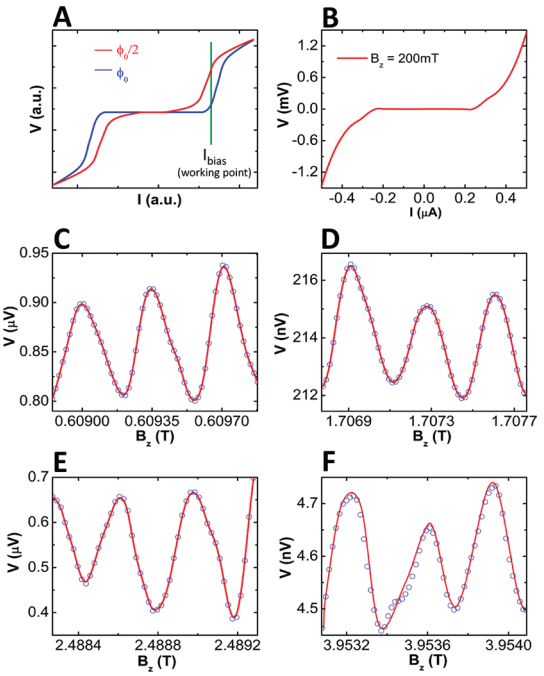

Figure 3. SQUID characteristics in perpendicular field configuration. (a) Schematic of two $I-V$ curves in the non-hysteretic regime of the device for an applied magnetic flux of Φ_0 and $\Phi_0/2$. By current biasing the device at the green line we can record the oscillation in the output voltage as the applied magnetic field is swept. (b) $I-V$ characteristic when the SQUID is in the non-hysteretic regime. (c−f) SQUID oscillations at various field ranges (C, 0.6; D, 1.7; E, 2.5; F, 4 T). The average oscillation period is 0.32 mT, consistent to what is observed at low magnetic field. Red lines in the figures are guides to the eyes.

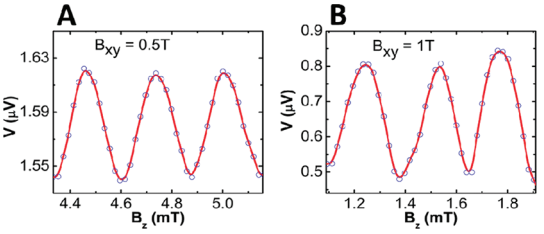

Figure 4. SQUID characteristics in parallel field configuration. (a and b) The voltage oscillations of the SQUID when a constant magnetic field is applied parallel to the SQUID plane and perpendicular to both the weak links. Red lines in the figures are guides to the eyes. To detect the oscillation a small probing field is applied perpendicular to the SQUID plane.

has to be extremely small (of the order of few nanometers), a feature which drastically reduces the critical current. On the other hand, operating standard μ-SQUIDs in perpendicular field reduces severely the operational field range well below 1 T. Here we demonstrate that μ-SQUIDs made from boron-doped diamond do not suffer from such limitations and can be operated in magnetic fields as high as 4 T even when applied in perpendicular configuration. This is more than a 6-fold increase on the present state of the art.[34]

Applying a large magnetic field (**B** > 500 mT) to a superconductor reduces the critical current. When the reduction of the critical current is below the value of the retrapping current, the voltage−current characteristics become non-hysteretic as schematically shown in Figure 3a and experimentally in Figure 3b. In this case, an ac measurement technique can be used to measure the SQUID oscillations as explained in the methods section. In Figure 3c−f we have shown the characteristic SQUID oscillations at various fields up to 4 T. The oscillations are not perfectly periodic because we had to use the *z*-coil (perpendicular to SQUID plane) for both, to apply the steady magnetic field (up to 4 T) and also to probe the SQUID oscillations (of the order of 0.3 mT). The field resolution is hence limited by the resolution of the magnet power supply (∼0.1 mT).[35] This could be improved by adding an additional feed line next to the μ-SQUID to probe the SQUID oscillations independently.[7]

To demonstrate the insensitivity of our SQUID to the applied field direction we have also measured SQUID oscillations by applying a constant field with a vector magnet in the $x-y$ plane (parallel to SQUID plane). In this configuration the SQUID oscillations were probed

using a small magnetic field of a few milli-Teslas in the *z*-coil. The voltage oscillations for a parallel field of 0.5 and 1 T, the maximal field achievable with our vector coil, are shown in Figure 4. Let us also emphasize that these oscillations were obtained for 300 nm thick superconducting boron-doped diamond layers. In this case the aspect ratio is very favorable for vortex penetration, and in standard superconductors, current oscillations are usually not observed in μ-SQUIDS for layers thicker than a few nanometers. The fact that we are able to observe SQUID oscillations for such geometries may originate from the granularity of the material,[36] which favors vortex pinning.

Let us mention that the resulting SQUID oscillations at high magnetic field have not been optimized at each field and for this reason the oscillation amplitude does not follow the field strength.[37] Here we simply demonstrate the proof of principle that a diamond SQUID can be operated at high magnetic field and this being independent of the field direction. To optimize the sensitivity of the diamond SQUID, it would be extremely interesting to employ single crystal diamond where higher critical currents[38] as well as higher critical fields ($\sim$10 T)[6] can be achieved.

SQUID oscillations surviving at high magnetic fields, independent of field orientation, open the possibility to exploit these exceptional properties for HF magnetic surface probe techniques.[2] Combining these exceptional superconducting and outstanding mechanical properties makes this monolithic system a highly promising tool, in particular for the detection of quantum motion in a diamond-based nanomechanical oscillator when inserted within one arm of a diamond SQUID.[7]

METHODS

Film Deposition. Prior to deposition, the wafers were cleaned by standard RCA SC1 solution and rinsed with deionized water in an ultrasonic bath. Immediately after rinsing, the wafers were immersed in a colloid of monodisperse diamond nanoparticles known to have a mean size of 6 nm and agitated by ultrasound for 30 min. Following this seeding process, the wafers were rinsed again with deionized water, blown dry in nitrogen, and immediately placed inside the growth chamber which was pumped down to a vacuum lower than 10^{-6} mbar. The chamber was then purged with hydrogen gas and a plasma ignited with 4% methane and 6500 ppm of trimethylboron diluted by hydrogen (better than 99.9999999% pure). The pressure was ramped to 50 mbar and the temperature was 700 °C as measured by optical pyrometry.

Electronic Measurements. The SQUID measurements were performed by current biasing the squid loop *via* a thermostable 1 MΩ resistor using a 16 bit NI-USB-6229 DAC. At low magnetic field, the $I-V$ characteristic is hysteretic as seen in Figure 2b and the SQUID oscillation is measured by recording the critical current as a function of magnetic field. The critical current is determined when a voltage drop is generated across the SQUID due to its transition from the superconducting to the normal state. The voltage is amplified with a NF-LI75a low-noise voltage amplifier and recorded *via* a Keithley 2000 multimeter. The SQUID oscillations shown in Figure 2 were obtained with a single $I-V$ curve at a fixed magnetic field. No averaging has been done.

At high magnetic field the SQUID is biased with a square wave signal by mixing a sinusoidal voltage (amplitude of 1 V and a frequency of 11.7 Hz) with the dc voltage of the NI-DAC. The voltage generated across the SQUID is amplified with a homemade ultralow noise voltage amplifier (0.5nV/(Hz)$^{1/2}$) and measured with a lock-in amplifier (Signal Recovery 7265). An $I-V$ curve measured with this technique is displayed in Figure 3b. By adjusting the DC voltage of the DAC, the bias current I_B can then be set at the working point of the SQUID (see Figure 3A). Sweeping the magnetic field at fixed bias current results in voltage oscillations as shown in Figure 3c–f and Figure 4a,b.

Acknowledgment. We would like to acknowledge technical assistance from the Nanofab team of the Institut Néel, in particular B. Fernandez. We also acknowledge valuable discussions with Wolfgang Wernsdorfer, Klaus Hasselbach, and Vincent Bouchiat and technical assistance from Y. Baines. This work has been supported by the French National Agency (ANR) in the frame of its program in "Nanosciences and Nanotechnologies" (SUPERNEMS Project no. ANR-08-NANO-033). This work was partially supported by the Fraunhofer Attract award "Hybrid HF-MEMS Filters for GHz-Communication and capillary MEMS systems for chemical and bio-chemical sensing, COMBIO".

REFERENCES AND NOTES

1. Cleuziou, J.-P.; Wernsdorfer, W.; Bouchiat, V.; Ondarçuhu, T.; Monthioux, M. Carbon Nanotube Superconducting Quantum Interference Device. *Nat. Nanotechnol.* **2006**, *1*, 53–59.
2. Kirtley, J. R.; Tsuei, C. C.; Sun, J. Z.; Chi, C. C.; Yu-Jahnes, Lock See; Gupta, A.; Rupp, M.; Ketchen, M. B. Symmetry of the Order Parameter in the High-T_c Superconductor $YBa_2Cu_3O_{7-\Delta}$. *Nature* **1995**, *373*, 225–228.
3. Wu, C. T.; Falco, C. M. High-Temperature Nb_3Sn Thin-Film SQUID'S. *Appl. Phys. Lett.* **1977**, *30*, 609–611.
4. Dilorio, M. S.; de Lozanne, A.; Beasley, M. R. High-TcSNS DC SQUIDs Produced by Electron Beam Lithography. *IEEE Trans. Magn.* **1983**, *19*, 308.
5. Rogalla, H.; David, B.; Rühl, J. Thin Film Nb_3Ge DC-SQUID with High Operating Temperature. *J. Appl. Phys.* **1984**, *55*, 3441.
6. Takano, Y. Superconductivity in CVD Diamond Films. *J. Phys.: Condens. Matter* **2009**, *21*, 253201.
7. Etaki, S.; Poot, M.; Mahboob, I.; Onomitsu, K.; Yamaguchi, H.; van der Zant, H. S. J. Motion Detection of a Micromechanical Resonator Embedded in a D.C. SQUID. *Nat. Phys.* **2008**, *4*, 785–788.
8. Ekimov, E. A.; Sidorov, A. A.; Bauer, E. D.; Mel'nik, N. N.; Curro, N. J.; Thompson, J. D.; Stishov, S. M. Superconductivity in Diamond. *Nature* **2004**, *428*, 542–545.
9. Blase, X.; Bustarret, E.; Chapelier, C.; Klein, T.; Marcenat, C. Superconducting Group-IV Semiconductors. *Nat. Mater.* **2009**, *8*, 375–382.
10. Nesladek, M.; Tromson, D.; Mer, C.; Bergonzo, P.; Hubik, P.; Mares, J. J. Superconductive B-doped Nanocrystalline Diamond Thin Films: Electrical Transport and Raman Spectra. *Appl. Phys. Lett.* **2006**, *88*, 232111.
11. Dubitskiy, G. A.; Blank, V. D.; Buga, S. G.; Semenova, E. E.; Kul'bachinskii, V. A.; Krechetov, A. V.; Kytin, V. G. Superhard Superconducting Materials Based on Diamond and Cubic Boron Nitride. *JETP Lett.* **2005**, *81*, 260–263.
12. Williams, O. A.; Kriele, A.; Hees, J.; Wolfer, M.; Müller-Sebert, W.; Nebel, C. E. High Young's Modulus in Ultrathin Nanocrystalline Diamond. *Chem. Phys. Lett.* **2010**, *495*, 84–89.
13. Gaidarzhy, A.; Imboden, M.; Mohanty, P.; Rankin, J.; Sheldon, B. W. High Quality Factor Gigahertz Frequencies in Nanomechanical Diamond Resonators. *Appl. Phys. Lett.* **2007**, *91*, 203503.

14. O'Connell, A. D.; Hofheinz, M.; Ansmann, M.; Bialczak, R. C.; Lenander, M.; Lucero, E.; Neeley, M.; Sank, D.; Wang, H.; Weides, M.; *et al*. Quantum Ground State and Single-Phonon Control of a Mechanical Resonator. *Nature* **2010**, *464*, 697–703.
15. Teufel, J. D.; Li, D.; Allman, M. S.; Cicak, K.; Sirois, A. J.; Whittaker, J. D.; Simmonds, R. W. Circuit Cavity Electromechanics in the Strong-Coupling Regime. *Nature* **2011**, *471*, 204–208.
16. Teufel, J. D.; Donner, T.; Li, D.; Harlow, J. W.; Allman, M. S.; Cicak, K.; Sirois, A. J.; Whittaker, J. D.; Lehnert, K. W.; Simmonds, R. W. Sideband Cooling Micromechanical Motion to the Quantum Ground State. *Nature* **2011**, *475*, 359–363.
17. Naik, A.; Buu, O.; LaHaye, M. D.; Armour, A. D.; Clerk, A. A.; Blencowe, M. P.; Schwab, K. C. Cooling a Nanomechanical Resonator with Quantum Back-Action. *Nature* **2006**, *443*, 193–196.
18. Knobel, R. G.; Cleland, A. N. Nanometre-Scale Displacement Sensing Using a Single Electron Transistor. *Nature* **2003**, *424*, 291–293.
19. Regal, C. A.; Teufel, J. D.; Lehnert, K. W. Measuring Nanomechanical Motion with a Microwave Cavity Interferometer. *Nat. Phys.* **2008**, *4*, 555–560.
20. Williams, O. A.; Douheret, O.; Daenen, M.; Haenen, K.; Osawa, E.; Takahashi, M. Enhanced Diamond Nucleation on Monodispersed Nanocrystalline Diamond. *Chem. Phys. Lett.* **2007**, *445*, 255–258.
21. Williams, O. A.; Nesladek, M.; Daenen, M.; Michaelson, S.; Hoffman, A.; Osawa, E.; Haenen, K.; Jackman, R. B. Growth, Electronic Properties and Applications of Nanodiamond. *Diamond Relat. Mater.* **2008**, *17*, 1080–1088.
22. Mandal, S.; Naud, C.; Williams, O. A.; Bustarret, E.; Omnès, F.; Rodière, P.; Meunier, T.; Saminadayar, L.; Bäuerle, C. Nanostructures Made from Superconducting Boron-Doped Diamond. *Nanotechnology* **2010**, *21*, 195303.
23. Anderson, P. W.; Dayem, A. H. Radio-Frequency Effects in Superconducting Thin Film Bridges. *Phys. Rev. Lett.* **1964**, *13*, 195–197.
24. Likharev, K. K. Superconducting Weak Links. *Rev. Mod. Phys.* **1979**, *51*, 101–159.
25. Skocpol, W. J. Critical Currents of Superconducting Microbridges. *Phys. Rev. B* **1976**, *14*, 1045–1051.
26. Courtois, H.; Meschke, M.; Peltonen, J. T.; Pekola, J. P. Origin of Hysteresis in a Proximity Josephson Junction. *Phys. Rev. Lett.* **2008**, *101*, 067002.
27. Hasselbach, K.; Mailly, D.; Kirtley, J. R. Micro-superconducting Quantum Interference Device Characteristics. *J. Appl. Phys.* **2002**, *91*, 4432–4437.
28. Hasselbach, K.; Veauvy, C.; Mailly, D. MicroSQUID Magnetometry and Magnetic Imaging. *Phys. C* **2000**, *332*, 140–147.
29. Voss, R. F.; Laibowitz, R. B.; Broers, A. N.; Raider, S. I.; Knoedler, C. M.; Viggiano, J. M. Ultra-Low-Noise Nb DC SQUIDS. *IEEE Trans. Magn.* **1981**, *17*, 395–399.
30. Rabaud, W.; Saminadayar, L.; Mailly, D.; Hasselbach, K.; Benoît, A.; Etienne, B. Persistent Currents in Mesoscopic Connected Rings. *Phys. Rev. Lett.* **2001**, *86*, 3124–3127.
31. Bluhm, H.; Koshnick, N. C.; Bert, J. A.; Huber, M. E.; Moler, K. A. Persistent Currents in Normal Metal Rings. *Phys. Rev. Lett.* **2009**, *102*, 136802.
32. Wernsdorfer, W.; Sessoli, R. Quantum Phase Interference and Parity Effects in Magnetic Molecular Clusters. *Science* **1999**, *284*, 133–135.
33. Chen, L.; Wernsdorfer, W.; Lampropoulos, C.; Christou, G.; Chiorescu, I. On-Chip SQUID Measurements in the Presence of High Magnetic Fields. *Nanotechnology* **2010**, *21*, 405504.
34. Finkler, A.; Segev, Y.; Myasoedov, Y.; Rappaport, M. L.; Ne'eman, L.; Vasyukov, D.; Zeldov, E.; Huber, M. E.; Martin, J.; Yacoby, A. Self-Aligned Nanoscale SQUID on a Tip. *Nano Lett.* **2010**, *10*, 1046–1049.
35. The low frequency noise observed in Figure 3c−f is due to slow thermal and temporal drifts of the magnetic power supply.The field values have been recorded by averaging the measured field value over a time period of approximately 1 min thus allowing the measurement of field values with less than 0.1 mT precision.
36. Dahlem, F.; Achatz, P.; Williams, O. A.; Araujo, D.; Bustarret, E.; Courtois, H. Spatially Correlated Microstructure and Superconductivity in Polycrystalline Boron-Doped Diamond. *Phys. Rev. B* **2010**, *82*, 033306.
37. The contrasts were not optimized in these experiments: to optimize the voltage oscillations one has to measure a complete current bias map, which means that for every bias current within the region where the red and blue curve form a S-shaped surface area (see figure 3A), one has to measure the voltage oscillations in order to find the best working point of the SQUID, which is a relatively time-consuming task. This has not been done here and hence the oscillation amplitudes do not follow the field dependence of the critical current.
38. Watanabe, M.; Kawano, A.; Kitagoh, S.; Yamaguchi, T.; Takano, Y.; Kawarada, H. Stacked SNS Josephson Junction of All Boron-Doped Diamond. *Phys. C* **2010**, *470*, S613–S615.